Bio-molecule-conjugated fluorescent organically modified silica nanoparticles as optical probes for cancer cell imaging

Jun Qian,[1] Xin Li,[1] Ming Wei,[1] Xiangwei Gao,[2] Zhengping Xu,[2] and Sailing He[1,*]

[1]*Centre for Optical and Electromagnetic Research, Zhejiang University; Joint Research Center of Photonics of the Royal Institute of Technology (Sweden) and Zhejiang University, Zijingang Campus, Zhejiang University, Hangzhou 310058, China.*

[2]*Bioelectromagnetics Laboratory, School of Medicine, Zhejiang University, Zijingang Campus, Hangzhou 310058, China.*

**Corresponding author: sailing@kth.se*

Abstract: Organically modified silica nanoparticles doped with Nile Red were synthesized and characterized. Silica encapsulation is relatively transparent for light and can protect hydrophobic Nile Red against denaturalization induced by the extreme bio-environment, making the entire nanoparticle hydrophilic and possess stable optical properties. The nanoparticles were conjugated with bio-molecules (such as apo-transferrin and folic acid), and our *in vitro* experiments revealed that these functionalized nanoparticles can serve as effective optical probes for specific targeting of cancer cells. As a preliminary study for future *in vivo* animal experiment, ORMOSIL nanoparticles were further co-conjugated with polyethyleneglycol (PEG) and apo-transferrin and the conjugates were also very good for *in vitro* targeting of HeLa cells. These bio-molecule functionalized ORMOSIL nanoparticles may serve as a robust tool for early diagnosis/therapy of cancer and other diseases.

OCIS codes: (160.2540) Fluorescent and luminescent materials; (160.4236) Nanomaterials; (300.6170) Spectra; (170.2520) Fluorescence microscopy; (170.3880) Medical and biological imaging.

References and links

1. P. N. Prasad, *Introduction to biophotonics*, (Wiley-Interscience, New York 2003).
2. P. N. Prasad, *Nanophotonics*, (Wiley-Interscience, New York 2004).
3. I. Roy, T. Y. Ohulchanskyy, D. J. Bharali, H. E. Pudavar, R. A. Mistretta, N. Kaur, and P. N. Prasad, "Optical tracking of organically modified silica nanoparticles as DNA carriers: a nonviral, nanomedicine approach for gene delivery," Proc. Natl. Acad. Sci. U.S.A. **102,** 279-284 (2005).
4. D. J. Bharali, I. Klejbor, E. K. Stachowiak, P. Dutta, I. Roy, N. Kaur, E. J. Bergey, P. N. Prasad, and M. K. Stachowiak, "Organically modified silica nanoparticles: a nonviral vector for in vivo gene delivery and expression in the brain," Proc. Natl. Acad. Sci. U.S.A. **102,** 11539-11544 (2005).
5. I. Roy, T. Y. Ohulchanskyy, H. E. Pudavar, J. E. Bergey, A. R. Oseroff, J. Morgan, T. J. Dougherty, and P. N. Prasad, "Ceramic-based nanoparticles entrapping water-insoluble photosensitizing anticancer drugs: a novel drug-carrier system for photodynamic therapy," J. Am. Chem. Soc. **125,** 7860-7865 (2003).
6. S. Kim, T. Y. Ohulchanskyy, H. E. Pudavar, R. K. Pandey, and P. N. Prasad, "Organically modified silica nanoparticles co-encapsulating photosensitizing drug and aggregation-enhanced two-photon absorbing fluorescent dye aggregates for two-photon photodynamic therapy," J. Am. Chem. Soc. **129,** 2669-2675 (2007).
7. T. Y. Ohulchanskyy, I. Roy, L. N. Goswami, Y. H. Chen, E. J. Bergey, R. K. Pandey, A. R. Oseroff, and P. N. Prasad, "Organically modified silica nanoparticles with covalently incorporated photosensitizer for photodynamic therapy of cancer," Nano Lett. **7,** 2835-2842 (2007).
8. S. Kim, H. Huang, H. E. Pudavar, Y. P. Cui, and P. N. Prasad, "Intraparticle energy transfer and fluorescence photoconversion in nanoparticles: an optical highlighter nanoprobe for two-photon bioimaging," Chem. Mater. **19,** 5650-5656 (2007).
9. S. Kim, H. E. Pudavar, A. Bonoiu, and P. N. Prasad, "Aggregation-enhanced fluorescence in organically modified silica nanoparticles: a novel approach toward high-signal-output nanoprobes for two-photon fluorescence bioimaging," Adv. Mater. **19,** 3791-3795 (2007).

#102094 - $15.00 USD Received 26 Sep 2008; revised 9 Nov 2008; accepted 10 Nov 2008; published 12 Nov 2008

10. A. Burns, H. Ow, and U. Wiesner, "Fluorescent core–shell silica nanoparticles: towards "lab on a particle" architectures for nanobiotechnology," Chem. Soc. Rev. **35,** 1028–1042 (2006).
11. M. Shimada, N. Shoji, and A. Takahashi, "Enhanced efficacy of bleomycin adsorbed on silica particles against lymph node metastasis derived from a transplanted tumor," Anticancer Res. **15,** 109-116 (1995).
12. X. Zhao, R. P. Bagwe and W. Tan, "Development of organic-dye-doped silica nanoparticles in a reverse microemulsion," Adv. Mater. **16,** 173-176 (2004).
13. M. Lal, L. Levy, K. S. Kim, G. S. He, X. Wang, Y. H. Min, S. Pakatchi, and P. N. Prasad, "Silica nanobubbles containing an organic dye in a multilayered organic/inorganic heterostructure with enhanced luminescence," Chem. Mater. **12,** 2632-2639 (2000).
14. T. K. Jain, I. Roy, T. K. De, and A. N. Maitra, "Nanometer silica particles encapsulating active compounds: a novel ceramic drug carrier," J. Am. Chem. Soc. **120,** 11092-11095 (1998).
15. C. Wang, Z. Ma, T. Wang, and Z. Su, "Synthesis, assembly, and biofunctionalization of silica-coated gold nanorods for colorimetric biosensing," Adv. Funct. Mater. **16,** 1673-1678 (2006).
16. J. Qian, K. T. Yong, I. Roy, T. Y. Ohulchanskyy, E. J. Bergey, H. H. Lee, K. M. Tramposch, S. He, A. Maitra, and P. N. Prasad, "Imaging pancreatic cancer using surface-functionalized quantum dots," J. Phys. Chem. B. **111,** 6969-6972 (2007).
17. K. T. Yong, J. Qian, I. Roy, H. H. Lee, E. J. Bergey, K. M. Tramposch, S. He, M. T. Swihart, A. Maitra, and P. N. Prasad, "Quantum rod bioconjugates as targeted probes for confocal and two-photon fluorescence imaging of cancer cells," Nano Lett. **7,** 761-765 (2007).
18. H. Ding, K. T. Yong, I. Roy, H. E. Pudavar, W. C. Law, E. J. Bergey, and P. N. Prasad, "Gold nanorods coated with multilayer polyelectrolyte as contrast agents for multimodal imaging," J. Phys. Chem. C. **111,** 12552-12557 (2007).
19. P. H. Yang, X. Sun, J. F. Chiu, H. Sun, and Q. Y. He, "Transferrin-mediated gold nanoparticle cellular uptake," Bioconjugate Chem. **16,** 494-496 (2005).
20. W. Jiang, A. Singhal, J. Zheng, C. Wang, and W. C. W. Chan, "Design and characterization of lysine cross-linked mercapto-acid biocompatible quantum dots," Chem. Mater. **18,** 4845-4854 (2006).
21. W. C. Chan, and S. Nie, "Quantum dot bioconjugates for ultrasensitive nonisotopic detection," Science **281,** 2016-2018 (1998).
22. Y. J. Lu, and P. S. Low, "Folate-mediated delivery of macromolecular anticancer therapeutic agents," Adv. Drug Del. Rev. **54,** 675-693 (2002).
23. C. P. Leamon, and P. S. Low, "Folate-mediated targeting: from diagnostics to drug and gene delivery," Drug Disc. Today. **6,** 44-51 (2001).
24. Y. J. Lu, E. Sega, C. P. Leamon, and P. S. Low, "Folate receptor-targeted immunotherapy of cancer: mechanism and therapeutic potential," Adv. Drug Del. Rev. **56,** 1161-1176 (2004).
25. S. A. Asher, S. F. Peteu, C. E. Reese, M. X. Lin, and D. Finegold, "Polymerized crystalline colloidal array chemical-sensing materials for detection of lead in body fluids," Anal. Bioanal. Chem. **373,** 632-638 (2002).
26. X. Gao, Y, Y. Cui, R. M. Levenson, L. W. K. Chung, and S. Nie, "In vivo cancer targeting and imaging with semiconductor quantum dots," Nat. Biotechno. **22,** 969-976 (2004).
27. B. Ballou, B. C. Lagerholm, L. A. Ernst, M. P. Bruchez, and A. S. Waggoner, "Noninvasive imaging of quantum dots in mice," Bioconjugate Chem. **15,** 79-86 (2004).
28. N. G. Khlebtsov, V. A. Bogatyrev , L. A. Dykman, and A.G. Melnikov, "Spectral extinction of colloidal gold and its biospecific conjugates," J. Colloid Interface Sci. **180,** 436-445 (1996).
29. B. N. Khlebtsov, V. A. Khanadeev, and N. G. Khlebtsov, "Determination of the size, concentration, and refractive index of silica nanoparticles from turbidity spectra," Langmuir **24,** 8964-8970 (2008).
30. H. C. Van de Hulst, *Light scattering by small particles,* (Wiley-Interscience, New York 1957).
31. G. S. He, P. P. Markowicz, T. C. Lin, and P. N. Prasad, "Observation of stimulated emission by direct three-photon excitation," Nature **415,** 767-770 (2002).
32. G. S. He, Q. Zheng, P. N. Prasad, J. G. Grote, and P. K. Hopkins, "Infrared two-photon-excited visible lasing from a DNA-surfactant-chromophore complex," Opt. Lett. **31,** 359-361 (2006).
33. K. E. Sapsford, L. Berti, and I. L. Medintz, "Materials for fluorescence resonance energy transfer analysis: beyond traditional donor-acceptor combinations," Angew. Chem. Int. Ed. **45,** 4562-4588 (2006).
34. C. Loo, A. Lowery, N. Halas, J. West, and R. Drezek, "Immunotargeted nanoshells for integrated cancer imaging and therapy," Nano Lett. **5,** 709-711 (2005).
35. X. Wu, H. Liu, J. Liu, K. N. Haley, J. A. Treadway, J. P. Larson, N. Ge, F. Peale, and M. P. Bruchez, "Immunofluorescent labeling of cancer marker Her2 and other cellular targets with semiconductor quantum dots," Nat. Biotechno. **21,** 41-46 (2003).
36. X. Huang, I. H. El-Sayed, and M. A. El-sayed, "Cancer cell imaging and photothermal therapy in the near-infrared region by using gold nanorods," J. Am. Chem. Soc. **128,** 2115-2120 (2006).

1. Introduction

Organic fluorophores with high quantum efficiency have not been applied widely in biological imaging area yet. The main obstacle is these fluorophores are hydrophobic, making them incompatible to aqueous biological systems. One approach to make the fluorophores

#102094 - $15.00 USD Received 26 Sep 2008; revised 9 Nov 2008; accepted 10 Nov 2008; published 12 Nov 2008

more biocompatible is to introduce more hydrophilic groups, such as ethylene-oxy or carboylic acid groups. However, the aggregations of the fluorophores can still be observed when they are incubated in cells. Another reason is that these fluorophores usually photobleach, as a result of denaturalization induced by the extreme bio-environment. It is therefore necessary to find solutions to overcome the above problems and apply organic fluorophores in bio-photonics areas.

During the past few years, organically modified silica (ORMOSIL) nanoparticles have been widely used in the applications of gene delivery as DNA carriers [1-4], Photodynamic Therapy (PDT) as drug carrier [5-7], and other photonics areas [8, 9]. ORMOSIL nanoparticles can usually encapsulate fluorophore or PDT drug, and have many advantages in bio-applications, such as (1) they are mesoporous, i.e. have bigger pores in their matrix (as compared to "pure" silica), which can facilitate some controlled release of encapsulated biomolecules like drugs and proteins, etc [5-7]; (2) they can be loaded with either hydrophilic or hydrophobic drugs/dyes: by changing the dye type, the fluorescent ORMOSIL nanoparticles can give good fluorescence quantum yield and tunable photoluminescence that spans the entire visible and IR spectrum [10]; by changing the drug type, the fluorescent ORMOSIL nanoparticles can be used to treat different kinds of diseases; (3) they can be surface-functionalized with various types of chemical groups, and can be further conjugated with different targeting bio-molecules; (4) they have less cytotoxicity and possess good biocompatibility [11-14].

Due to the ultra-small size and surface charge, ORMOSIL silica nanoparticles can be uptaken by cells through the "enhanced permeability and retention effect" (their surfaces carry positive charge and the membranes of the cancer cells usually carry negative charge). Based on this property, ORMOSIL nanoparticles have been utilized for applications of photodynamic therapy and gene delivery [3-7]. However, this uptake is non-specific, and it is very important in bio-applications to target specifically the disease cells. For example, in PDT applications, we want to kill the disease cells without killing together healthy cells during the treatment. In gene delivery, people utilize ORMOSIL nanoparticles to carry some DNA to certain cells (to play their functions) without releasing the DNA to other normal cells. It is particularly important to establish a bio-molecule-conjugated ORMOSIL nanoparticle platform to target specifically the disease cells for diagnosis/therapy applications.

In the present paper, we synthesized Nile Red doped and amino-group-functionalized ORMOSIL nanoparticles. Nile Red dyes emit red color fluorescence when they are excited in DMSO solution, but they are hardly water soluble and the fluorescence excited in aqueous solution is negligible. However, when Nile Red dyes are encapsulated in ORMOSIL nanoparticles, they can emit very strong red fluorescence when excited in a water environment. This property is very important for bio-applications since most bio-activities occur in a hydrophilic environment. The absorption and emission properties of Nile Red Dye before and after encapsulation were also characterized by absorbance spectrophotometer and photoluminescence (PL) spectroscopy, and almost no photobleaching could be observed after long time excitation, indicating nanoparticles possess stable optical properties. ORMOSIL nanoparticles were conjugated with apo-transferrin (Tf) and folic acid (FA) [15]. We used the ORMOSIL nanoparticle conjugates for *in vitro* targeting HeLa cell lines, which are well known to over-express the transferrin-receptor (TfR) [16-21] and folic acid receptors (FR) [22-25]. We also used the nanoparticles conjugates to treat with the COS-7 cell lines, where neither transferrin nor folic acid receptors are known to be over-expressed, and almost no uptake could be observed. Fluorescence microscopy imaging technique was used to confirm above receptor-mediated uptake. ORMOSIL nanoparticles were further co-conjugated with polyethyleneglycol (PEG, which can improve the long *in vivo* circulation of nanoparticles [26, 27]) and apo-transferrin, and the conjugates also showed a similar *in vitro* targeting of HeLa cells as compared with only apo-transferrin-conjugated nanoparticles. The PEG-Tf-co-conjugated ORMOSIL nanoparticles are good for use in future *in vivo* animal experiments as PEG can prevent the aggregation and improve the long circulation of nanoparticles besides reducing the non-specific targeting of nanoparticles during an *in vivo* experiment.

#102094 - $15.00 USD Received 26 Sep 2008; revised 9 Nov 2008; accepted 10 Nov 2008; published 12 Nov 2008

2. Materials and methods

2.1 Synthesis of Nile Red-loaded and amino-group-functionalized ORMOSIL nanoparticles

The ORMOSIL nanoparticles were synthesized in the nonpolar core of Aerosol-OT/DMSO/water micelles as discussed before. Typically, the micelles were prepared by dissolving a certain amount of Aerosol-OT and 1-butanol in 10 ml of DI water by vigorous magnetic stirring. 100 μl of Nile Red in DMSO (5 mM) was then added to the solution under magnetic stirring. Half an hour later, 150 μl of neat VTES was added to the micellar system, and the resulting solution was stirred for about 1 hour. Next, ORMOSIL nanoparticles were precipitated by adding 15 μl of APTES and stirred for another 20 h at room temperature. After the formation of the nanoparticles, surfactant Aerosol-OT, cosurfactant 1-butanol, residual VTES and APTES were removed by dialyzing the solution against DI water in a 12-14 kDa cutoff cellulose membrane for 50 h. The dialyzed solution was then filtered through a 0.45 μm cutoff membrane filter to be used in later experiments. By varying the concentrations of Aerosol-OT and VTES, different sizes of ORMOSIL nanoparticles could be achieved.

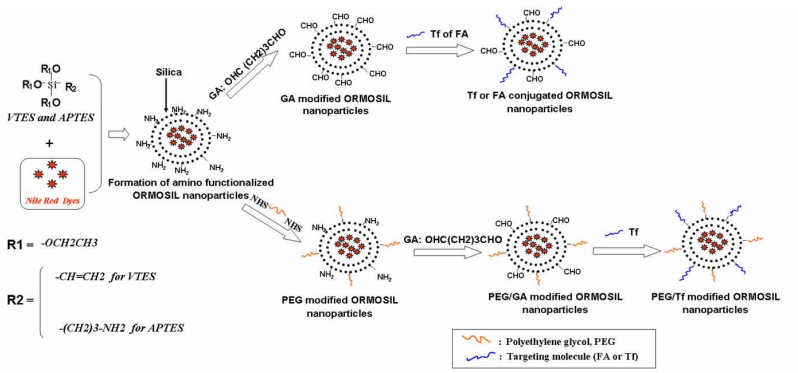

Fig. 1. Schematic illustration of our two routes for the bio-conjugation of ORMOSIL nanoparticles.

2.2 Conjugation with Bio-Molecules

Here the bio-conjugation of ORMOSIL nanoparticles was done in two routes for *in vitro* experiments (the second route can also be for future *in vivo* experiments). The upper route of Fig. 1 shows the scheme for transferrin/folic acid conjugation of ORMOSIL nanoparticles. ORMOSIL nanoparticle solution was dissolved in the equivalent volume of HEPES buffer (pH value ~8.0, 40 mM) to form stock solution A. Over-excess amount of GA was added to 4 ml stock solution A, and we let the reactions between GA and amino groups last for about 3 hours. The reacted solution was dialyzed against DI water to eliminate the unreacted excess GA molecules. The dialyzed solution was diluted to half concentration by HEPES buffer, and 4 mg transferrin/500 nmol FA was added to 1 ml as-diluted solution for conjugation. The reactions lasted for about 1 hour. Certain amounts of glycine were added to both bio-molecule-conjugated and non-bio-molecule-conjugated (only-GA-modified) nanoparticles to block the remaining aldehyde groups on the surface of nanoparticles. After purification, all the samples were stored at 4 ℃ for further cell treatment.

The nether route of Fig. 1 shows the scheme for the PEG-Tf-co-conjugation of ORMOSIL nanoparticles. 18 mg NHS-PEG-NHS (MW: 3,000) was added to 2.5 ml of the original ORMOSIL nanoparticle solution, and NaOH solution was added drop by drop to maintain the pH value of the solution around 8. 3 hours later, the reaction solution was dialyzed against DI water for 24 h to remove the unreacted excess NHS-PEG-NHS molecules. PEG-modified nanoparticle solution was dissolved in the equivalent volume of HEPES buffer to form stock solution B. Over-excess amount of GA was added to 4 ml stock solution B, and

#102094 - $15.00 USD Received 26 Sep 2008; revised 9 Nov 2008; accepted 10 Nov 2008; published 12 Nov 2008

the reaction lasted for about 3 hours. The reaction solution was then dialyzed against DI water to eliminate the unreacted excess GA molecules. 3 ~ 4 hours later, the dialyzed solution was diluted to half concentration by HEPES buffer, and 4 mg Tf was added to 1 ml as-diluted solution for conjugation. Certain amounts of glycine were added to both PEG-GA-modified and PEG-Tf-co-conjugated nanoparticles to block the remaining aldehyde groups on the surface of nanoparticles. After purification, all the samples were stored at 4 ℃ for further cell treatment.

2.3 Characterization

Transmission electron microscope (TEM) was taken by a JEOL JEM-1200EX transmission electron microscope operating at 160 kV in bright-field mode for ORMOSIL nanoparticles. A Shimadzu 2550 UV-vis scanning spectrophotometer at room temperature recorded the ultraviolet and visible (UV–vis) extinction spectra from 350 to 800 nm. The photoluminescence spectra were obtained by a Fluorescence Spectrophotometer (F-2500, HITACHI, Japan) with an excitation Xenon lamp ranging from 500 to 800 nm.

2.4 Cell culture

HeLa cells (human cancer cell lines) and COS-7 cells (derived from kidneys of African green monkeys) were cultivated in Dulbecco minimum essential media (DMEM) with 10% fetal bovine serum (FBS), 1% penicillin, and 1% amphotericin B. One day before the treatment, cells were seeded in 35 mm cultivation dishes at a confluence of 70-80 %. During the treatment, samples were added to the cell plates and the cell incubation process lasted for 2 hours at 37 ℃ with 5% CO_2. Then the cells were washed thrice with PBS and directly imaged with a Fluorescence Microscopy.

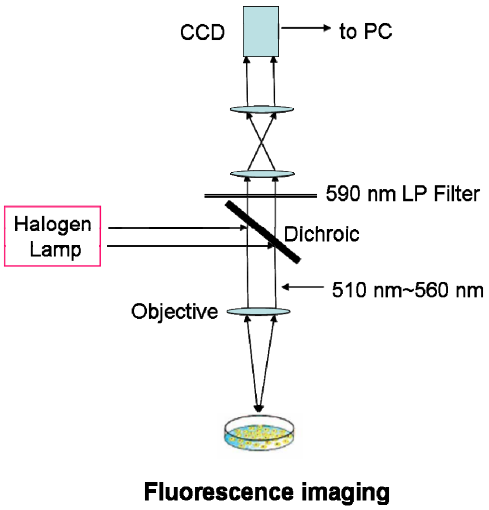

Fig. 2. Schematic illustration of the setup for fluorescence imaging.

2.5 Fluorescence Microscopy

Fluorescence imaging of cells was taken from a Nikon E200 microscope. Green light (510 nm-560 nm, obtained when white light coming from a Halogen lamp passed through a dichroic beam splitter), was used to excite the cell sample through the 40×/0.65 objective lens that also collected the fluorescence signal for imaging. After passing through a long-wavelength-pass optical filter (590 nm LP), all the fluorescence signals were received by the CCD, which was installed on the top of the microscope, and then transferred to a software in a PC.

#102094 - $15.00 USD Received 26 Sep 2008; revised 9 Nov 2008; accepted 10 Nov 2008; published 12 Nov 2008

3. Results and discussion

TEM images of the Nile Red-loaded ORMOSIL nanoparticles were shown in Fig. 3. These nanoparticles of four different sizes, which were all spherical in shape and highly monodispersed, have the average diameters of 15 nm, 35 nm, 55 nm and 85 nm. In bio-applications, small ORMOSIL nanoparticles are prone to entering the cells, while the big ones have large surface areas and thus can be modified by more types of functional groups and conjugated to more types of bio-molecules.

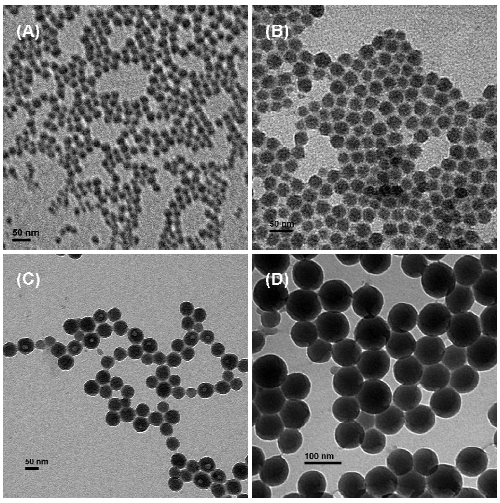

Fig. 3. TEM pictures of Nile Red-doped and amino-group-functionalized ORMOSIL nanoparticles with four different average diameters (From A to D: 15 nm, 35 nm, 55 nm and 85 nm).

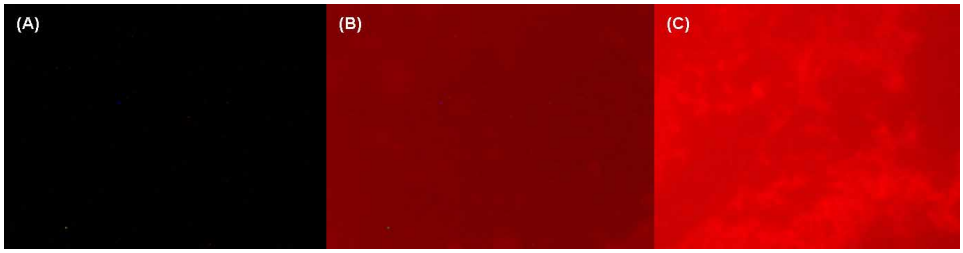

Fig. 4. Fluorescence imaging pictures of (A) glass slide, (B) glass slide with Nile Red aggregate, (C) glass slide with the aggregate of Nile Red-doped ORMOSIL nanoparticles.

The doping of Nile Red in the nanoparticles was proved by the fluorescence imaging. A drop of DMSO solution of Nile Red and a drop of aqueous solution of Nile Red doped nanoparticles were slowly evaporated on a glass slide. When they became dry, the fluorescence from the aggregates of the nanoparticles could be clearly observed in Fig. 4 (C), which was much brighter than the fluorescence from the aggregates of Nile Red powder, as shown in Fig. 4 (B). It could be concluded that the Nile Red molecules have been encapsulated in the silica nanoparticles (otherwise, the fluorescence from the aggregates of the nanoparticles should be as weak as that from the aggregates of Nile Red powder). The hydrophilic silica coating is relatively transparent for light, and can protect hydrophobic Nile Red against denaturalization induced by the environment, making the entire nanoparticle optically stable.

As shown in Fig. 5 (a), the extinction spectra of Nile Red in DMSO solution and the aqueous solution of Nile Red-loaded ORMOSIL nanoparticles (with an average diameter of 35 nm) were similar around their spectra peak (555 nm; this extinction peak is mainly due to

#102094 - $15.00 USD Received 26 Sep 2008; revised 9 Nov 2008; accepted 10 Nov 2008; published 12 Nov 2008

the absorption), while in the range of 350-450 nm, Nile Red-loaded ORMOSIL nanoparticles extincted more light than Nile Red in DMSO. The difference mainly arose from the Rayleigh scattering by the nanoparticles, since the ORMOSIL nanoparticles were about 35 nm in diameter (comparable to light wavelength) while Nile Red dye molecules in DMSO were only about 1 nm in diameter and their scattering effect was almost negligible. Since the scattering intensity is inverse proportional to λ^4 (λ is the optical wavelength), the scattering-induced extinction of nanoparticles in the range of 350-450 nm was more obvious than that in the long wavelength range. Note that absorption is much more obvious than scattering around 555 nm and thus the scattering-induced extinction is negligible (though exists) as compared with the absorption-induced extinction. To make the above discussion more convincing, we also did some quantitative analyses. A small silica particle (35 nm in diameter) possesses a complex refractive index $n = n' + i * n''$ .The particles are suspended in water with a refractive index [28]: $n_0 = 1.32334 + 3.479\times10^3/\lambda^2 - 5.111\times10^7/\lambda^4$ (1), where the wavelength is expressed in nm. To simulate the dye absorption, a Lorentzian peaked absorption spectrum is considered: $n''(\lambda) = a/\left[(\lambda - \lambda_{\max})^2 + b\lambda^2\right]^c$ (2), where a, b, and c are the fitting parameters, and $\lambda_{\max} = 555nm$ is the resonance wavelength. From the measured spectrum data, a, b, and c can be taken as b=0.02, c=3, and a=0.22x10^{12} for wavelengths expressed in (nm), and the normalized absorption spectrum of dye can be simulated according to Eq.(2) (green line in Fig. 5 (b)). For pure silica particles, the real part of the refractive index equals $n' = 1.475$ [29]. According to Mie theory [30], the extinction and scattering efficiency factors of dye encapsulated silica particles can be expressed as:

$$Q_{ext} = 4x\,\mathrm{Im}\left\{\frac{m^2-1}{m^2+2}\left[1+\frac{x^2}{15}\left(\frac{m^2-1}{m^2+2}\right)\frac{m^4+27m^2+38}{2m^2+3}\right]\right\} + \frac{8}{3}x^4\,\mathrm{Re}\left\{\left(\frac{m^2-1}{m^2+2}\right)^2\right\}, \quad Q_{sca} = \frac{8}{3}x^4\left|\frac{m^2-1}{m^2+2}\right|^2$$

Here $x = \pi d n_0(\lambda)/\lambda$ (d is the diameter of nanoparticle and equals to 35 nm), m is a complex relative refractive index, and $m(\lambda) = n_{silica}/n_{water} = (n'(\lambda) + iA\times n''(\lambda))/n_0(\lambda)$. From our experimental data, the fitting constant A = 0.001 was found, and the simulation results are shown in Fig. 5 (b) (Extinction: red line; scattering: blue line). The simulations are in excellent agreement with the measured spectra and our qualitative discussion. Note also that the simulated particle extinction peak is slightly blue-shifted (about 10 nm) as compared to the dye solution spectrum. In Fig. 5 (a), nanoparticles show virtually no extinction in the wavelength region of 650-800 nm, and this region is considered to be very useful for bio-imaging as an optical window due to the high penetration depth of light in tissue at these wavelengths. Combined with multi-photon excitation [31, 32] and Fluorescence Resonance Energy Transfer (FRET) [33] technologies, our Nile Red-loaded nanoparticles platform can have the potential applications in e.g. *in vivo* bio-imaging and photodynamic therapy.

Figure 5 (c) represents the fluorescence emission spectra of Nile Red in DMSO solution and the aqueous solution of Nile Red-loaded ORMOSIL nanoparticles. After encapsulated, the emission peak wavelength of Nile Red was 606 nm, which has a blue shift of about 18 nm as compared with that of Nile Red in DMSO solution. The reason for the blue shift is not so clear so far [it may be attributed to the types of solvent (the nanoparticles were in water, and the dyes were in DMSO), and/or because the intra-particle environment affected the emission property of dye molecules]. The red fluorescence coming from Nile Red was still clear enough to be distinguished in the bio-imaging experiment.

As shown in Fig. 5 (d), after excited by 532 nm-light (power density: ~10 mW/cm^2) for half an hour, the photoluminescence intensity of Nile Red-loaded ORMOSIL nanoparticles still kept very well. Almost no photobleaching could be observed after the long time excitation, indicating the as-synthesized nanoparticles possess stable optical properties, which is very useful for long time dynamic bio-imaging.

#102094 - $15.00 USD Received 26 Sep 2008; revised 9 Nov 2008; accepted 10 Nov 2008; published 12 Nov 2008

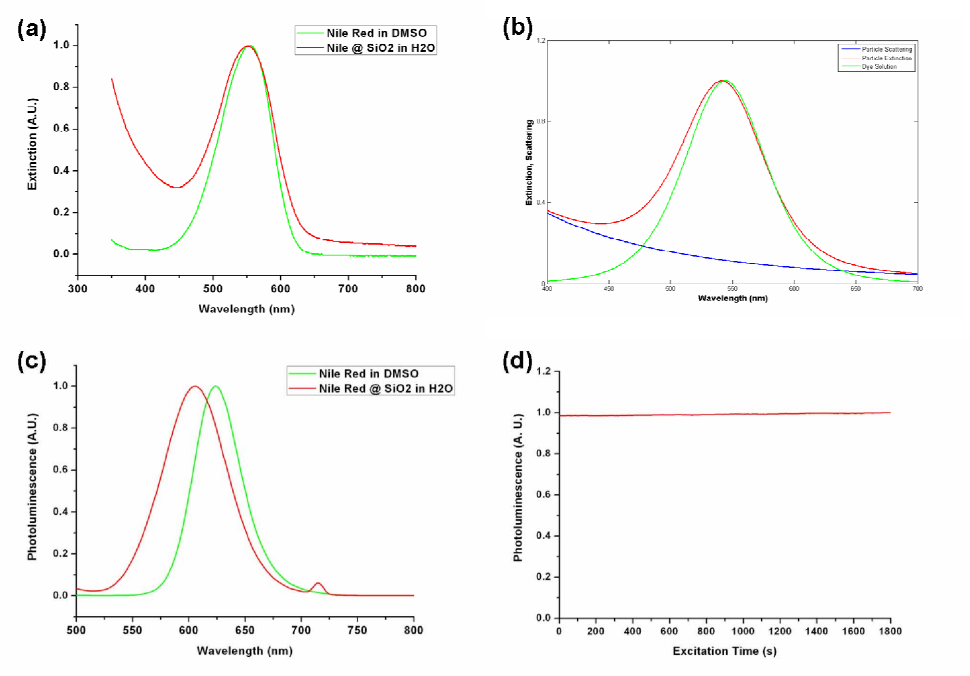

Fig. 5. Experimental extinction (a), simulated extinction (b) and fluorescence emission spectra (c) of Nile Red in DMSO solution and the aqueous solution of Nile Red-loaded ORMOSIL nanoparticles. (d): Time trace of photoluminescence intensity of Nile Red-loaded ORMOSIL nanoparticles, which was excited by 532 nm-light (power density: ~10 mW/cm^2) for half an hour.

Figure 6 shows the fluorescence imaging of the HeLa cells and COS-7 cells, which were treated by (only-) amino-group-functionalized nanoparticles. It could be clearly seen from the fluorescence imaging that, the bright red fluorescence (which was emitted from Nile Red) covered both types of cells quite well and the targeting was very strong and uniform. However, the uptake was through the "enhanced permeability and retention effect", and both the cancer (HeLa) cells and non-cancer (COS-7) cells could be targeted nonspecifically by the nanoparticles. It is therefore particularly important to establish a bio-molecule-conjugated ORMOSIL nanoparticle platform to target specifically the disease cells (without targeting healthy cells) for diagnosis/therapy applications.

After conjugated with bio-molecules (transferrin/folic acid), ORMOSIL nanoparticles were utilized for the specific targeting of cancer cells. Fluorescence microscopy imaging technique was used to image the HeLa cells which were treated with different types of nanoparticles. As shown in Fig 7, non-bio-molecule-conjugated nanoparticles could not been uptaken by the HeLa cells. Since the amino groups on the surface of nanoparticles have been completely terminated by the GA molecules and the surface charges of nanoparticles changed accordingly, nanoparticles could not been uptaken through the "enhanced permeability and retention effect". However, bio-molecule-conjugated nanoparticles (both Tf conjugated and FA conjugated) stained the HeLa cells with high efficiency (the bright red fluorescence covered HeLa cells very well). This is a result of receptor-mediated uptake of these bio-molecule-conjugated nanoparticles with their corresponding receptors (TfR/FR), which are known to be over-expressed on the surface of HeLa cells (active targeting).

#102094 - $15.00 USD Received 26 Sep 2008; revised 9 Nov 2008; accepted 10 Nov 2008; published 12 Nov 2008

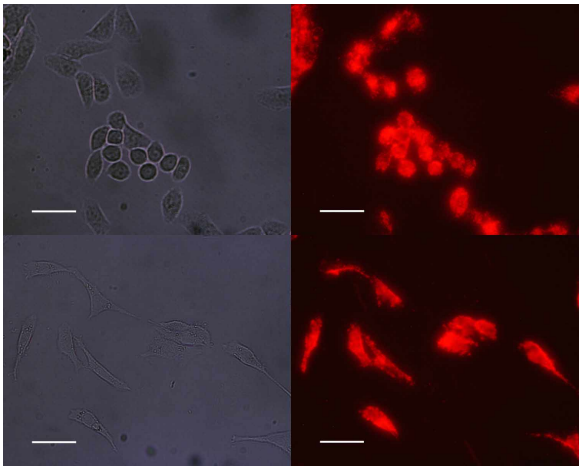

Fig. 6. Fluorescence imaging pictures of HeLa cells (Upper row) and COS-7 cells (Bottom row) treated with amino-group-functionalized nanoparticles. The panel on the left displays the transmission images of cells, and their corresponding fluorescence images are shown in the right panel. The scale bar is 50 μm.

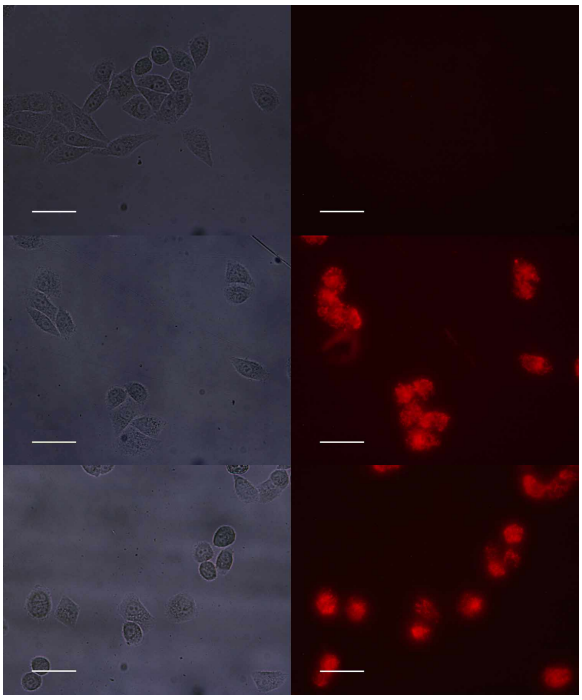

Fig. 7. Fluorescence imaging pictures of HeLa cells treated with non-bio-molecule-conjugated nanoparticles (Upper row), Tf-conjugated nanoparticles (Middle row), and FA-conjugated nanoparticles (Bottom row). The panel on the left displays the transmission images of cells, and their corresponding fluorescence images are shown in the right panel. The scale bar is 50 μm.

#102094 - $15.00 USD Received 26 Sep 2008; revised 9 Nov 2008; accepted 10 Nov 2008; published 12 Nov 2008

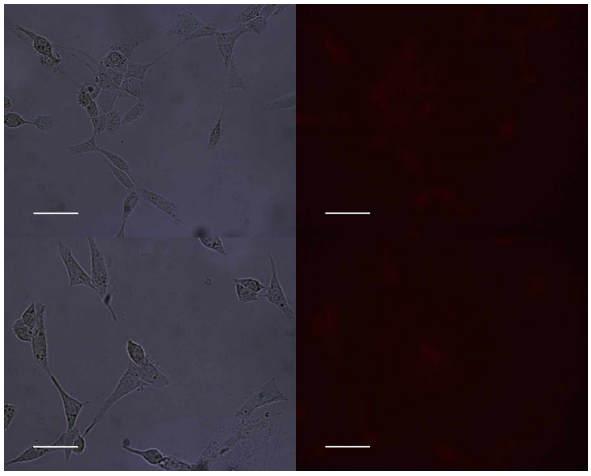

Fig. 8. Fluorescence imaging pictures of COS-7 cells treated with Tf-conjugated nanoparticles (Upper row) and FA-conjugated nanoparticles (Bottom row). The panel on the left displays the transmission images of cells, and their corresponding fluorescence images are shown in the right panel. The scale bar is 50 μm.

To confirm the uptake of Tf/FA-conjugated nanoparticles in HeLa cell lines is mediated by the Tf/FA receptors, comparative studies of Tf-conjugated and FA-conjugated nanoparticles were carried out in the COS-7 cell lines, which are lack of Tf and FA receptors. As shown in Fig. 8, the uptake of both Tf-conjugated nanoparticles and FA-conjugated nanoparticles could hardly be observed in COS-7 cell lines, as compared with the robust uptake of the same batch of bio-conjugated nanoparticles by the HeLa cells. These control experiments confirmed the receptor-mediated uptake of these bio-conjugated nanoparticles in HeLa cell lines.

From above fluorescence imaging results (Figs. 6-8), we can conclude that (only-) amino-group-functionalized nanoparticles could be uptaken nonspecifically by both cancer cells and non-cancer cells (Fig. 6). However, bio-molecule-conjugated ORMOSIL nanoparticles could target specifically the cancer cells without targeting healthy cells (Figs. 7 and 8), and such a discrimination ability of our method will be helpful to the diagnosis/therapy for certain diseases.

For PEG-Tf co-conjugation, we used separately amino-group-functionalized, PEG-modified, PEG-GA-modified, and PEG-Tf-co-conjugated nanoparticles to treat the HeLa cell lines, and the imaging results were shown in Fig. 9. As shown in pictures A and B, PEG-modified nanoparticles have less passive uptake as compared with amino-group-functionalized nanoparticles [the red fluorescence (which was emitted from Nile Red, and covered the HeLa cells) in picture B was slightly dimmer than that in picture A]. Besides, no aggregation was observed in our *in vitro* imaging experiment (otherwise, a big chunk of very bright fluorescence may appear in picture B), which is very helpful to the future *in vivo* experiment. PEG-GA-modified nanoparticles show no passive uptake in the HeLa cells as seen in picture C. In picture D, PEG-Tf-co-conjugated nanoparticles show specific targeting of the HeLa cells (with picture C as the control), and the targeting was very similar to that of HeLa cells treated with Tf-conjugated nanoparticles. This *in vitro* experiment was carried out here as a preliminary study for our further *in vivo* animal experiment. PEG can prevent the aggregation (improve the long circulation of nanoparticles) and also reduce the non-specific targeting of nanoparticles during an *in vivo* experiment. It is necessary to assess the positive uptake function of PEG-Tf-co-conjugated nanoparticles in *in vitro* experiments prior to their *in vivo* applications. In our future work, ORMOSIL nanoparticles will also be co-conjugated with PEG and certain antibodies (instead of Tf) which are more specific to certain disease cell

#102094 - $15.00 USD Received 26 Sep 2008; revised 9 Nov 2008; accepted 10 Nov 2008; published 12 Nov 2008

lines. We will test PEG's special functions in *in vivo* experiment, and apply the conjugates for *in vivo* diagnosis and therapy.

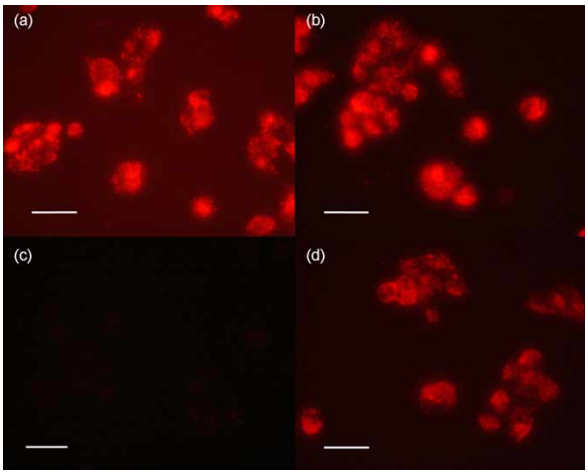

Fig. 9. Fluorescence imaging pictures of HeLa cell lines, treated separately with amino-group-functionalized (A), PEG-modified (B), PEG-GA-modified (C), and PEG-Tf-co-conjugated nanoparticles (D). The scale bar is 50 μm.

4. Conclusion

Fluorescent organically modified silica nanoparticles, doped with water-insoluble organic dyes, and surface-functionalized with amino groups, have been synthesized. The nanoparticles have a uniform and tunable size distribution, and can be formulated as a stable aqueous dispersion. The nanoparticles possess stable optical properties and have been further conjugated with Tf and FA, whose receptors are over-expressed in HeLa cells but not in COS-7 cells. Tf and FA conjugated nanoparticles show excellent specific targeting of HeLa cells but almost no uptake in COS-7 cells, which confirm the receptor-mediated uptake of these bio-conjugated nanoparticles in HeLa cell lines. PEG and Tf have further been co-conjugated with nanoparticles, and the conjugates also show a good positive uptake in *in vitro* cell imaging. This experiment of PEG-Tf-co-conjugated nanoparticles was carried out here as a preliminary study for our future *in vivo* animal experiment. Certain DNA molecules, antibodies [like anti-Her2, whose receptors are over-expressed in breast cancer cells (SKBr3) [34, 35], or anti-EGFR, whose receptors are over-expressed in malignant oral epithelial cell lines (HOC 313 clone8 and HSC 3) [36]] and drugs (like photosensitizer for PDT application) can also be utilized in our system of ORMOSIL nanoparticles. The present multifunctional nanoparticles will have prospective applications in e.g. bio-sensor, *in vivo* bio-imaging and bio-therapy.

Acknowledgments

This work was supported partially by a multidisciplinary project of Zhejiang University and the Swedish Foundation for Strategic Research (SSF). The authors are grateful to one of the reviewers for making some quantitative simulation to compare with our experimental results.

#102094 - $15.00 USD Received 26 Sep 2008; revised 9 Nov 2008; accepted 10 Nov 2008; published 12 Nov 2008